

1 **Tuning Organic Crystal Chirality by Enantiomer-Specific**
2 **Oriented Attachment**

3 Jingren Li ^{a,b}, Yanbo Liu ^{a,b}, Zhiqiang Guo ^c, Dandan Han ^{a,b*} and Junbo Gong ^{a,b}

4 *^a School of Chemical Engineering and Technology, State Key Laboratory of Chemical*
5 *Engineering, Tianjin University. Tianjin, 300072, P. R. China*

6 *^b Haihe Laboratory of Sustainable Chemical Transformations, Tianjin, 300192, P.R.*
7 *China*

8 *^c Jewim Pharmaceutical (Shandong) Co., Ltd., Shandong, 271000, P.R. China*

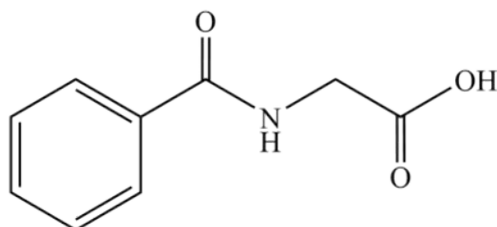
9
10
11
12
13
14
15
16
17
18
19
20
21
22
23
24

*Corresponding author.

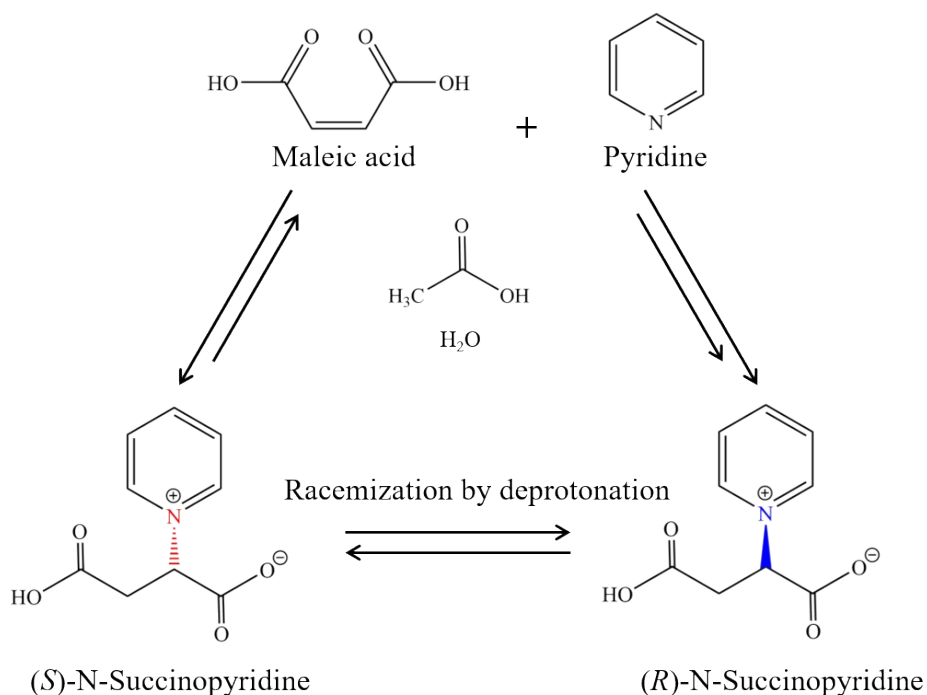
*E-mail address: handandan@tju.edu.cn (Dandan Han).

25 **Chemicals**

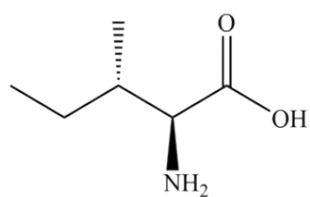
26 N-benzoylglycine (CAS no. 495-69-2, purity \geq 99.0 %) and maleic acid (CAS no.
27 110-16-7, purity \geq 99.0 %) were purchased from Tianjin Heowns Biochemistry
28 Technology Co. LTD of China. L-isoleucine (CAS no. 73-32-5, purity \geq 99.0 %), L-
29 leucine (CAS no. 61-90-5, purity \geq 99.0 %), L-valine (CAS no. 72-18-4, purity \geq
30 99.0 %), and pyridine (CAS no. 110-86-1, purity \geq 99.0 %) were purchased from
31 Shanghai Aladdin Biological Co. LTD of China. All of the chemicals were used
32 without further purification. Ultrapure water (resistivity = 18.2 M Ω cm) was prepared
33 in our laboratory using the NANOPURE system from BARNSTEAD (Thermo
34 Scientific Co., China).



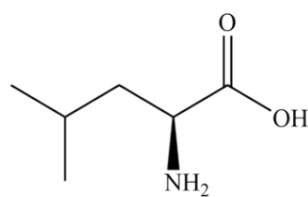
35
36 **Fig. S1** Chemical structure of N-benzoylglycine.



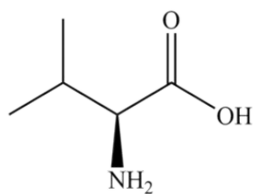
38
39 **Fig. S2** Aza-Michael addition of pyridine to maleic acid.



L-Isoleucine



L-Leucine



L-Valine

40

41

Fig. S3 Chemical structure of L-Isoleucine, L-Leucine and L-Valine.

42

43

44

45

46

47

48

49

50

51

52

53

54

55

56

57

58

59

60 *Detailed Experimental Procedures*

61 **1. Viedma Ripening:** The sample of commercially available N-benzoylglycine
62 powder (0.25 g) was suspended in a saturated solution of 1 mL distilled water using a
63 sealed round-bottom flask (5 mL). Grinding medium (3.0 g of 0.8 mm YTZ zirconia
64 ceramic beads) was added and the sample was stirred at 1500 rpm with a magnetic
65 stirring bar (10 mm×4 mm, oval). Slurry samples (ca. 100 μ L) were collected at
66 regular intervals using an automatic pipet and deposited on filter paper to dry, and
67 then analyzed through CD. After each sample, an equal volume of saturated solution
68 was replenished to the round-bottomed flask.

69 **2. Synthesis of N-succinopyridine:** A solution of maleic acid (11.9 g, 10.24 mol) and
70 1.0 equiv. of liquid pyridine (8.1 g, 10.24 mol) and water (8 mL) was stirred in a
71 sealed crystallizer using an oval magnetic stir bar at 90 °C. After a large number of
72 white crystals appeared in the clarified solution, acetic acid (12 mL) was added. The
73 solution was then stirred and kept in suspension at the same temperature for several
74 days and finally filtered to obtain white N-succinopyridine crystals.

75 **3. Crystallization through Slow Evaporation:** Single crystals of N-succinopyridine
76 were grown by slow evaporation of water from a Petri dish (10 cm diameter). N-
77 succinopyridine (ca. 10 g) was dissolved in distilled water (50 mL) at room
78 temperature with stirring and subsequently covered with perforated aluminum foil to
79 slow evaporation. Slow crystallization of large single crystals occurred over several
80 days. Crystals typically measured 1 x 0.5 x 0.25 cm.

81 **4. Boiling Experiments:** Boiling experiments were performed using a round
82 bottomed flask (100 mL). Ground N-benzoylglycine (ca. 30 g) was dissolved in water
83 (20 mL) in a round bottom flask. The mixture was refluxed at 180 °C for about 6-24 h
84 until aggregate formation was observed. The size of the aggregates ranged from 0.2
85 cm to 1 cm in diameter (20 mg to 1.5 g in mass). For N-succinopyridine, the
86 formation of large aggregates was clearly observed by refluxing approximately 15 g
87 dissolved in 10 mL of water at 160 °C for 15-24 h.

88 For the three amino acids of the racemic compounds, mainly isoleucine as an

89 example, ZnO (ca. 3 g) and DL-isoleucine (ca. 3 g) dissolved in the volume ratio of
90 60% ethanol aqueous solution (ca. 15 mL) were added to a round-bottomed flask (100
91 mL), and refluxed for 6-12 h at a temperature of 120 °C. Formation of large
92 aggregates of the conglomerate containing ZnO was clearly observed.

93 **5. Circular Dichroism:**

94 **N-benzoylglycine:** Solid-state circular dichroism was used to quantify the crystal
95 enantiomeric excess (CEE) of N-benzoylglycine aggregates obtained during the
96 Viedma ripening process as well as in boiling experiments. CD spectra were recorded
97 from 240 to 350 nm using a MOS-500 circular dichroism spectrometer. The
98 resolution of 5 points/nm was used and each curve generated was the average of 3 or
99 5 accumulations collected at a scan rate of 50 nm/min. Solid samples of N-
100 benzoylglycine were prepared as KBr pellets. N-benzoylglycine was ground with a
101 mortar and pestle, KBr pellets were prepared by adding 50 mg of potassium bromide
102 crystals (concentration 2.0% wt/wt) to the mortar, mixing the sample until a
103 homogeneous mixture was obtained, and then this mixture was vacuum-pressed at ca.
104 8 tons for ca. 20 s to form a translucent and homogeneous pellet. The sample
105 assembly is mounted using a standard circle cell holder with the sample placed as
106 close to the detector as possible.

107 **N-succinopyridine:** As we tested the circular dichroism chromatogram of
108 synthesized N-succinopyridine, we did not find any significant characteristic peaks in
109 the region of 200-800 nm, whereas there was a significant signal in the near-infrared
110 band at 800-900 nm. Therefore, for the circular dichroism chromatogram of N-
111 succinopyridine, we tested it using a Jasco J-1700 circular dichroism spectrometer in
112 the near-infrared band. Pure chiral samples of the standards were obtained by
113 cultivating single crystals with a bandwidth of 20 nm for testing, sample and
114 potassium bromide concentrations of 3.0% wt/wt, and other conditions were the same
115 as those for benzoylglycine.

116 **6. Calibration Curves:** The crystal enantiomeric excess (CEE) of viedma ripening
117 and N-benzoylglycine aggregates was determined using a calibration curve. The
118 enantiomeric excess (% ee) of the crystalline samples was calculated using Equation 1,

119 where $x_{(+)}$ and $x_{(-)}$ are the weights of CD-positive and CD-negative crystals,
120 respectively.

121
$$\text{enantiomeric excess (\%)} = \frac{x_{(+)} - x_{(-)}}{x_{(+)} + x_{(-)}} \times 100\%$$

122 (1)

123 Samples with varying enantiomeric excess are prepared by mixing appropriate
124 proportions of levo- and dextro-crystallized powders while maintaining a constant
125 total weight. The calibration curve is generated by plotting the CD signal at a
126 specified wavelength (260 nm) against the enantiomeric excess of the standard. For
127 each standard, multiple pellets are prepared and measured to determine the average
128 CD signal and standard deviation (typically $n = 3$). The calibration curve was then
129 used to determine the enantiomeric excess of the samples in the boiling experiment.
130 Pure chiral samples used as standards for the construction of calibration curves were
131 obtained by viedma ripening, and the chiral purity of the Vviedma ripening samples
132 was continuously determined by circular dichroism until the peak spectral signals
133 determined by sampling two adjacent time intervals were essentially unchanged, such
134 that we considered the viedma ripening to have proceeded completely and pure
135 enantiomers of a single chirality were obtained.

136 **7. Scanning electron microscopy:** SEM images were obtained using an Field
137 Emission Scanning Electron Microscopy (Apreo S LoVac, Thermo Fisher Scientific)
138 operating at 15 keV acceleration voltage. The samples were fixed on glass slides (7.5
139 cm x 2.5 cm) using double-sided conductive tape. An MSP-1S Magnetron Sputter was
140 used to apply a gold layer (ca. 10 nm) on the samples prior to imaging.

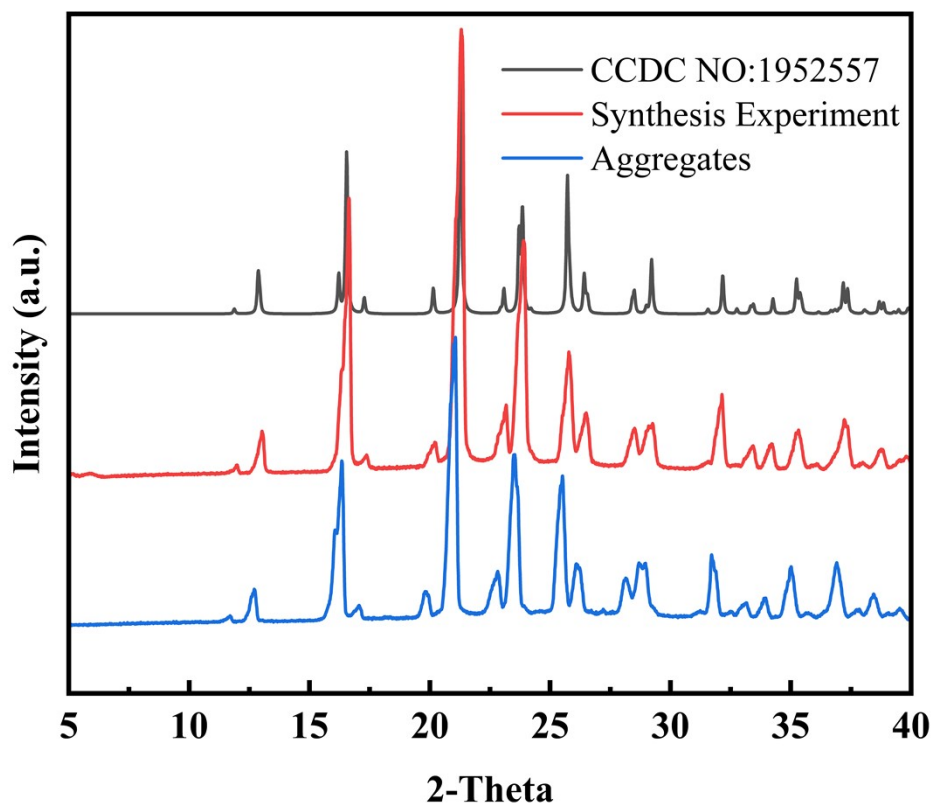
141 **8. Powder x-ray diffraction (PXRD):** Powder XRD of the milled crystals was
142 determined using a powder X-ray diffractometer (Rigaku MiniFlex 600, Rigaku,
143 Japan) by Cu. $K\alpha$ radiation (1.54046 Å) at 40 kV and 100 mA, with diffraction angles
144 (2θ) in the range of 2-40° , and scanning rate of 8°/min.

145 **9. High performance liquid chromatography (HPLC) assay:** The enantiomeric
146 excesses in the amino acid aggregates were determined by a Waters 2695 series high

147 performance liquid chromatograph (HPLC). The chromatographic analysis was
148 performed on a MCI GEL CRS10W column (50×4.6 mm, $3 \mu\text{m}$) at $25 \text{ }^\circ\text{C}$ with a UV
149 detection wavelength of 256 nm , and the mobile phase was a 1% (by mass
150 concentration) copper sulfate salt solution at a flow rate of 1.0 mL/min .

151 **10. Thermal analysis:** Simultaneous thermogravimetric analysis (TGA) was
152 performed on a TGA/DSC 3+/1100 SF thermal balance (Mettler-Toledo) and
153 differential scanning calorimetry (DSC) on a DSC 1 differential scanning calorimeter
154 (Mettler-Toledo) with sample volumes ranging from 4 mg to 8 mg . All measurements
155 were carried out under dynamic nitrogen protection (airflow 25 mL/min) and heated
156 at a constant rate of $10 \text{ }^\circ\text{C/min}$ to $400 \text{ }^\circ\text{C}$ or $600 \text{ }^\circ\text{C}$.

157



158

159 Figure S4. The X-ray powder diffraction patterns of the N-Succinopyridine crystals and
160 aggregates we prepared, and the simulated X-ray crystallographic diffraction pattern of N-
161 Succinopyridine from its single crystal structure (CCDC: 1952557).

162



163

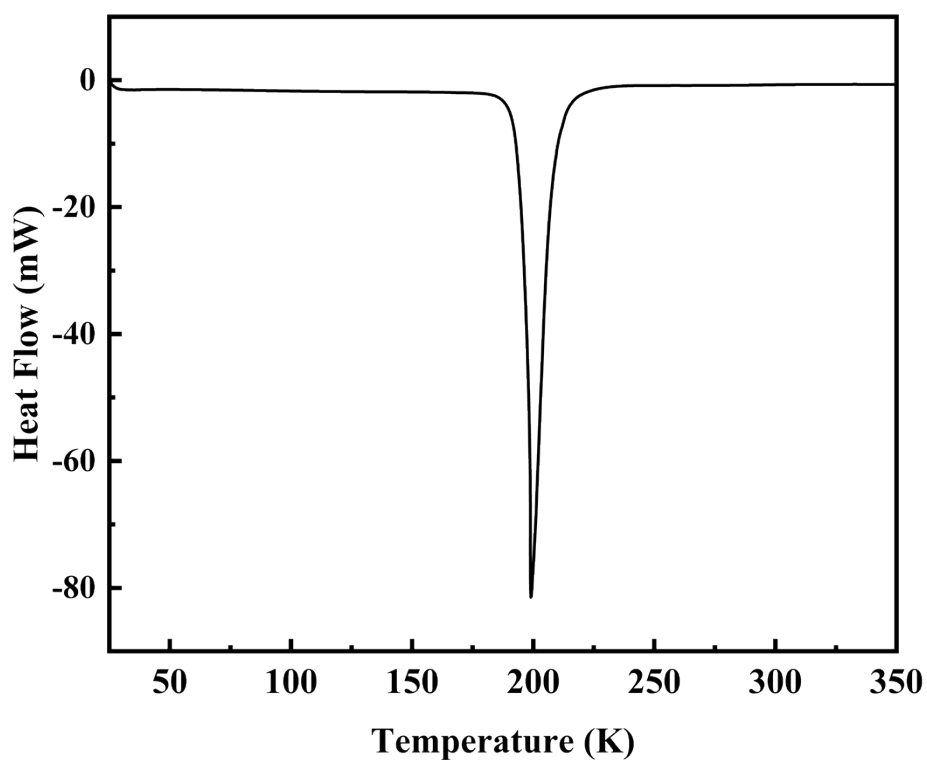
164

Fig. S5 Microphotographs of the single crystals of (*R*)-N-Succinopyridine

165

and (*S*)-N-Succinopyridine.

166



167

Fig. S6 DSC shows heat flow response of N-succinopyridine.

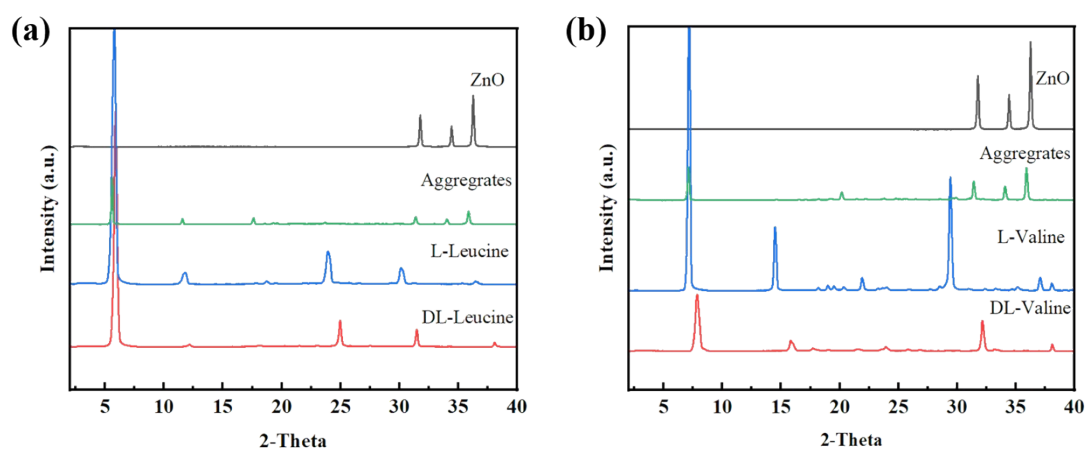
168

169 *Notes:* After synthesizing N-succinopyridine, we obtained by DSC test that it starts

170 melting at a temperature of about 180 °C, so in the case of water as a solvent, we need

171 to preferably 160 °C while maintaining the ability to boil.

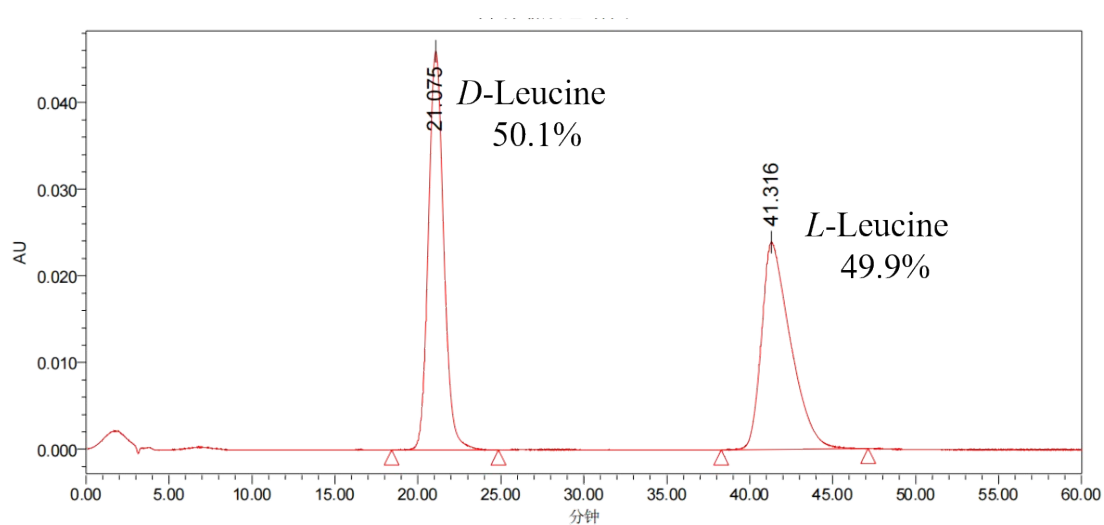
172



173

174 **Fig. S7** (a) XRD pattern of the pure DL-leucine, L-leucine, ZnO and the aggregates. (b) XRD
175 pattern of the pure DL-valine, L-valine, ZnO and the aggregates.

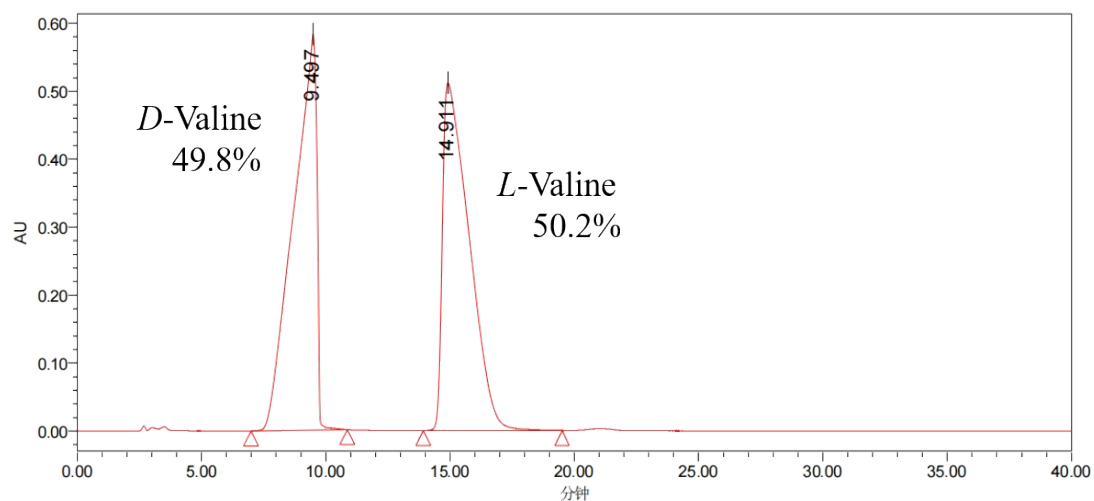
176



177

178 **Fig. S8** Liquid chromatographic detection of DL-leucine crystal aggregates formed in the presence
179 of zinc oxide.

180

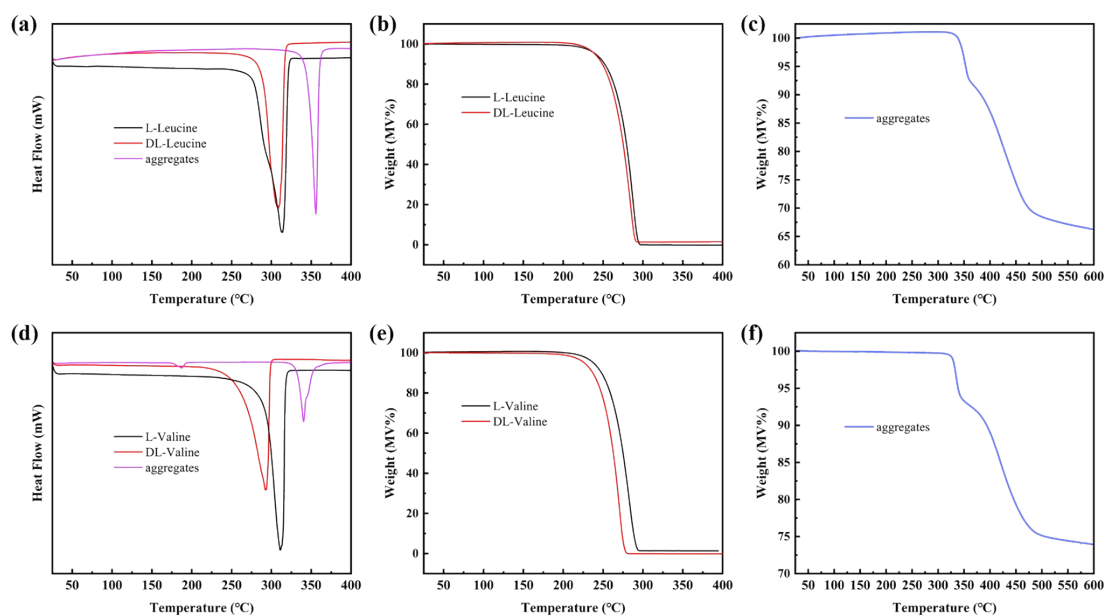


181

182 **Fig. S9** Liquid chromatographic detection of DL-valine crystal aggregates formed in the presence

183

of zinc oxide.



184

185 **Fig. S10** (a) TGA showing thermal response of DL-leucine, L-leucine and the aggregates. (b) (c)

186 DSC shows heat flow response of DL-leucine, L-leucine and the aggregates. (d) TGA showing

187 thermal response of DL-valine, L-valine and the aggregates. (e) (f) DSC shows heat flow response

188

of DL-valine, L-valine and the aggregates.